Bulletin of Glaciological Research 24 (2007) *1–11*

Article

Interannual variation of summertime precipitation over the Qilian Mountains in Northwest China

Akiyo YATAGAI
Research Institute for Humanity and Nature, Kamigamo-Motoyama, Kita-ku, Kyoto 603–8047, Japan

(Received September 20, 2005; Revised manuscript accepted November 10, 2006)

Abstract

To better understand the time-space structure of the interannual variation of precipitation in the summer time, hereafter meaning June to August (JJA), in the Qilian Mountain region, an empirical orthogonal function (EOF) analysis is applied to the summertime precipitation times for 41 years (1961–2001) over there. The atmospheric circulation field, the moisture transport and the precipitation patterns associated with the dominant mode is shown by using European Centre for Medium-range Weather Forecast (ECMWF) reanalysis (ERA40, 1.125 degree grid) dataset and a new precipitation dataset which expresses an orographic enhancement of precipitation.

The first mode of the analysis, which explained 24.8% of the total precipitation variance, had a single mode centered along the Hexi Corridor region of this mountainous region with a weak increasing trend of precipitation. The second mode, which explained 15.8% of the total variance, had a dipole structure between the Hexi Corridor (north of 38°N) and the region south of this corridor. This mode was correlated with the Indian Summer Monsoon Rainfall (IMR), and the northern part of the Qilian Mountains had a negative correlation to IMR. The third mode had a dipole structure between the Tibetan Plateau area and the northern desert area. The westerly circulation anomaly was the dominant factor to define the wet (much precipitation) or dry (less precipitation) years around the Qilian Mountains. The second mode, which had a significant negative correlation with the IMR, was also related to the westerly circulation anomaly. In the southern part of the Qilian Mountains, a pressure anomaly around the western plateau area and the southwesterly moisture flux were also related to the interannual variation of the precipitation anomaly in this region.

1. Introduction

Analyses of ice core samples from glaciers in high-mountain regions of the mid-latitudes help researchers understand the past climates of these regions. In particular, many ice core samples from the mountains in the high-elevation Tibetan Plateau have been analyzed (*e.g.,* Thompson *et al.,* 1988, 1989, 1990, 2000). Since summertime is a major accumulation season with a lot of precipitation and it is easy to make out inter-annual signals in the ice samples, it is important to better understand the interannual variation of the precipitation in the mountain areas. In spite of the importance, the characteristics and dominant factor of the interannual variation of the precipitation over such a region have yet to be clarified.

The summer time precipitation and melting snow is an important source of water for the Tibetan Plateau region, particularly in the arid and semi-arid areas where the water used for sustaining ecological and human society. Therefore, it is crucial to estimate the precipitation quantitatively, and to understand the dynamical processes those affect variations in the precipitation over the mountainous regions of the Tibetan Plateau. In this study, we focus on the Qilian Mountains of the Tibetan Plateau. This region is shown in Fig. 1. It is located in the upper reach of the Yellow River and the Heihe River. Therefore, this paper aims to clarify the time-space structure of the interannual variability of summer precipitation over and around the Qilian Mountains for the hydrologists who study the hydrological budget or hydrological resources management there as well as glaciologists who interpret the past environment from the ice cores records etc (Nakawo *et al.,* 2002; Nakawo and Sakai, 2006).

Summertime precipitation in the northwest part

of China is affected by both the westerly circulation system and the southerly monsoon system. Recent meteorological reanalysis data has revealed that the northeast part of the Tibetan Plateau and northeast China receives moisture from the northwest and from the south (Yatagai and Yasunari 1998; Yatagai, 2003). This is supported by a study with an atmospheric general circulation model (GCM) (Numaguti, 1999) as well as column integrated moisture source analysis that included water isotope partitioning (Yoshimura *et al.,* 2004). Further analysis by using more sophisticated models or finer resolution reanalysis dataset may lead to better understanding of the ice core records. This kind of approach should be efficient to understand the origin of water in the ice cores.

Another way to gain an understanding of the interannual signals in the ice cores is to know dominant factors of the interannual variation of the precipitation. Over such a complicated region, it is important to investigate the dynamical effects on precipitation including tele-connections. The tele-connections and precursor signals are not always explained dynamically. However, precursor signals are used for seasonal predictions and strong simultaneous correlations helps to project the relationships between the sporadic proxy data.

Many studies have found that the tele-connections affect monsoon rainfall over China (*e.g.,* Ding 1994). However, most analyses have been made for the plain regions of China, namely east of 110°E, not the mountainous regions, due to the small amount of local observation data in the mountains. Over the semi-arid regions in the north and northwest part of China, some studies revealed the relationship between El-Nino/Southern Oscillation (ENSO) or Indian summer monsoon circulation (Wang and Li, 1990; Yatagai and Yasunari, 1995; Feng and Hu, 2004). However, for the Qilian Mountains in the northeast part of the Tibetan Plateau, the causes and the characteristics of the interannual variation of summertime precipitation remains unclear.

Yatagai and Yasunari (1995) investigated the regionality of the interannual variation of summer time precipitation over the regions that includes Taklimakan, Jungar, Mongolia, and northern China, and found that Taklimakan shows a negative correlation to the Indian summer monsoon rainfall (IMR), whereas Loess Plateau shows a positive correlation to IMR. Recently, Feng and Hu (2004) pointed out the role of the Indian summer monsoon as a "facilitator" that connects ENSO with northern China rainfall. Further, recently, several studies showed that the Indian summer monsoon-ENSO relationship has been varied (Kumar *et al.,* 1999; Wang *et al.,* 2001). Therefore, it is important to investigate the interannual variation of summer time precipitation in and around the Qilian Mountains, and their relation of this variation to the Indian summer monsoon.

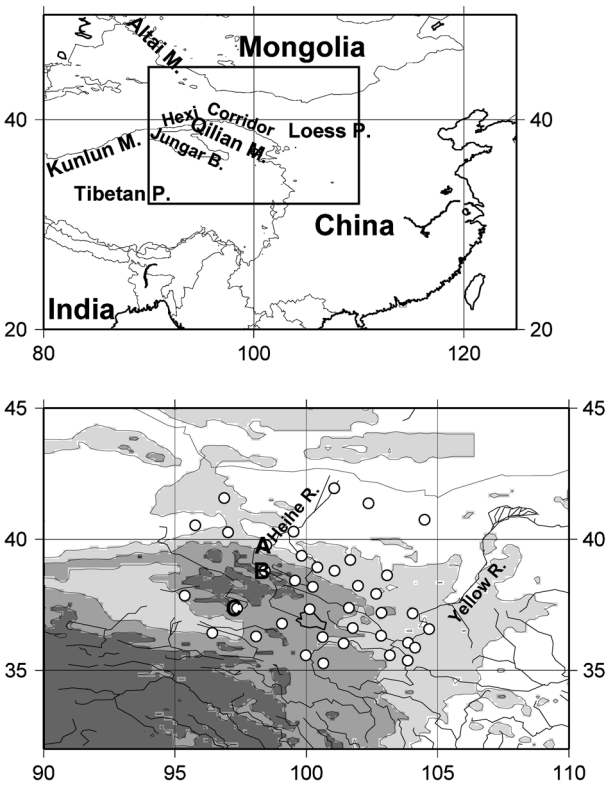

Fig. 1. The study region. The initial are as follows: M=mountains, P=plateau, B=basin, R=river. Inner rectangle in the upper map is the area for the lower map. The upper map contours are 3000 m, whereas those in the lower map are 1500 m. In the lower map, the shaded regions are elevations exceeding 1500, 3000, and 4500 with the darkest being highest, and the open circles mark locations of the 41 stations used for an empirical orthogonal function (EOF) analysis.

For this study, we used a 41-year (1961–2001) precipitation dataset from stations in the northeast part of the Tibetan Plateau and its adjacent regions (Fig. 1) to investigate the time-space structure of the variations in the summertime precipitation, meaning that in June, July, and August (JJA). Then, atmospheric circulation anomalies related to the interannual variability was investigated. The relationship between the Indian summer monsoon and the areal precipitation over and around the Qilian Mountains was also investigated by using a recent rain-gauge-based grid precipitation dataset that represents the orographic effect of precipitation.

2. Data

The following data sets were used in this study.

(1) Monthly precipitation data from 116 stations over the region [90–110°E/32–45°N] of China for the period 1961–2001. These daily precipitation datasets were

compiled by the China Meteorological Administration. In this study we used the data after summing the daily precipitation at each station for the 92 days of summertime. Among these stations, we used the data from the 37 stations that are within latitudes 95–105°E and longitudes 35–43°N (Fig. 1) for EOF analysis. The location of the stations and the geographical features around the study region are also shown in Fig. 1.

(2) Monthly all-India rainfall data for the period 1961–2001. These data were obtained from the Indian Institute of Tropical Meteorology (Parthasarathy *et al.* 1995). We calculated the total summertime rainfall in India to examine the correlation in precipitation between India and the target region (hereafter, IMR).

(3) East Asia gauge-based daily precipitation analysis. Xie *et al.* (2004, 2006) describes a new gauge-based dataset of daily precipitation on a 0.5° lat/lon grid over the East Asia region of 65–150°E and 5–60°N, which expresses orographic enhancement of precipitation (hereafter, the Base product). The set of the product also includes 0.1° lat/lon grid product over the Yellow River domain as a derived product (hereafter, the Derived product). From this dataset, we used the Base product for the period 1961–2001, and the Derived product for the period 1978–1997. The Base product covers the land area of the domain [65–150°E/5–60°N] for 1978–2001. From 1961–1977, the Base product covers only over China. In addition, we used daily precipitation climatology in a 0.05 degree grid which was created as an inter-mediate product to make the Base/Derived product. Yatagai *et al.* (2005) used this climatology dataset to validate a 20 km mesh general circulation model precipitation, because the other well-known grid precipitation product have not been represented precipitation climatology well enough to validate such hi-resolution model result.

The basic algorithm of creating the above dataset is a modification of Chen *et al.*'s (2002) method for creating monthly grid precipitation data by using an optimum interpolation (OI) technique. One of the major improvements of this modification is the following. To express the orographic effect where the station data is not available, the new algorithm used the monthly climatology that was adjusted using the parameter-elevation regressions on independent slopes model (PRISM) (Daly *et al.* 1994). The model was applied to monthly climatology data from China and Mongolia in order to express the orographic effect where the station data is not available. Details are shown in Xie *et al.* (2006). The data source for the Base/Derived products are from the State Meteorological Administration and the Yellow River Commission, which had data reporting rates that exceeded 90%. For the earlier period, 1961–1977, we used only data from the State Meteorological Administration was used.

(4) European Centre for Medium Range Weather Forecasts (ECMWF) 40-Year Reanalysis (ERA40). We used data on the vertically integrated water vapor flux and its divergence and the grid spacing is 1.125 degree grid. The monthly mean upper-air atmospheric data analysis has 2.5 degree grid spacing, and this data was used to diagnose the large-scale atmospheric circulation field. The period for 1961–2001 is used in this study.

3. Climatology and Trend

Figure 2 shows the summertime (JJA) mean (1978–2002) vertically integrated water vapor flux and its

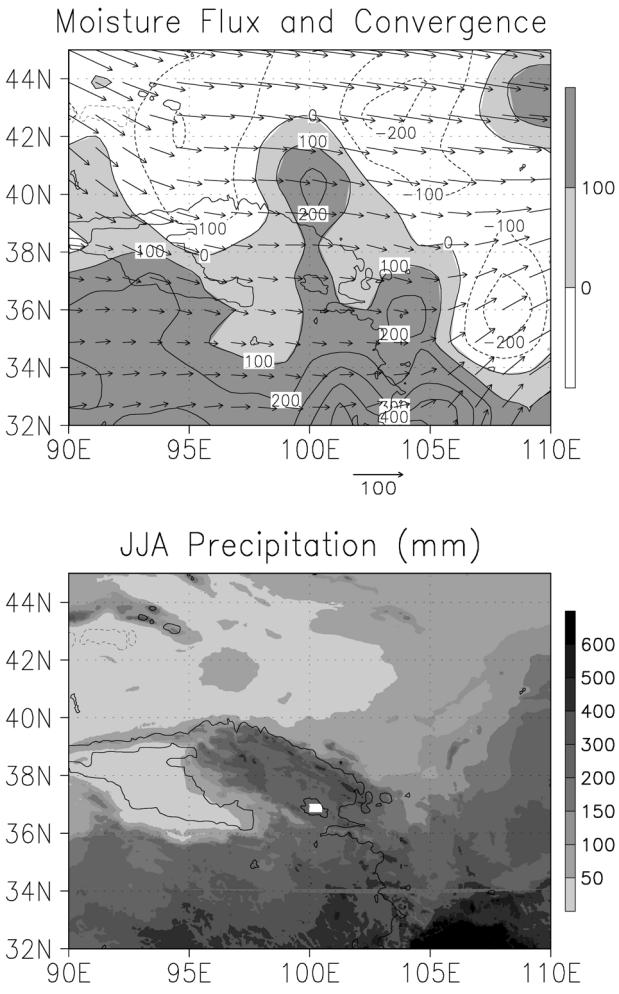

Fig. 2. Moisture patterns for summertime (JJA) 1978–2002. Upper diagram: climatological mean vertically integrated water vapor flux (kg m^{-1} s^{-1}) and its convergence (kg m^{-2} per three months). The shading marks regions with convergence. Lower diagram: East Asia gauge-based precipitation climatology (mm per three months). The solid line is the 3000-m elevation contour, which bounds the Tibetan Plateau.

convergence. The moisture convergence (shaded region) shows where the precipitation exceeds evapotranspiration. The overall characteristics are the same with those of Yatagai and Yasunari (1998) and Yatagai (2003) (which showed the climatological moisture transport field by using ECMWF 15 years dataset (ERA15) in 2.5 degree horizontal resolution). Over the Qilian Mountains, the summer time mean moisture flows from the west. A day-to-day moisture flow pattern varies by the atmospheric circulation field, sometimes it comes from the northwest and sometimes it comes from the southwest according to the position of trough/ridge in mid-latitude (Yatagai and Yasunari, 1998). It is interesting to see that a maximum convergence is observed at 100°E/40°N, where is the basin of the Heihe River (Fig. 1). The East Asia gauge-based precipitation climatology (Fig. 2, lower diagram) shows a clear precipitation maximum over the Qilian Mountains (95–102°E/36–40°N). Comparing the convergence pattern with that of precipitation, places of convergence maxima and precipitation maxima are not always the same. Since a convergence means total area averaged and seasonal (JJA) averaged precipitation exceeds evapotranspiration. In arid/semi-arid region, most precipitation may evaporate in a short period. This results in convergence of 0 mm. If we have solid precipitation in mountain areas and/or precipitation is stored as snow or in a water reserver, seasonal maxima of precipitation and convergence do not appear simultaneously (Yatagai, 2003).

Although recent earth observation systems reveal global precipitation pattern including mountain areas and in various times scales including diurnal change, observed precipitation patterns and its variability of the Qilian Mountains has not been clarified. Since our target region is out of Tropical Rainfall Measuring Mission (TRMM) observation area, a gestational meteorological satellite provides us information on diurnal convection, which is a dominant circulation characters in mountain areas. A clear diurnal variation is observed in upper tropospheric humidity (UTH) pattern over this area (Yatagai, 2001). More UTC is observed in the evening (12 UTC) than the morning (00 UTC) over the Qilian Mountains and less UTC is observed around the Tibetan Plateau (higher than 3000 m, above sea level) within the distance about 500 km. The southern foot of the Qilian Mountians is still on the Tibetan Plateau and is not as low as that of northern foot. Therefore, major moisture source of the precipitation in both northern and southern slopes of the Qilian Mountains may differ depends on the atmospheric circulation field including diurnal change. Detail analysis between precipitation and moisture transport is necessary in the future by using datasets with enough resolution in time and space, and isotope observation. In this paper, we compare the characteristics of interannual variation

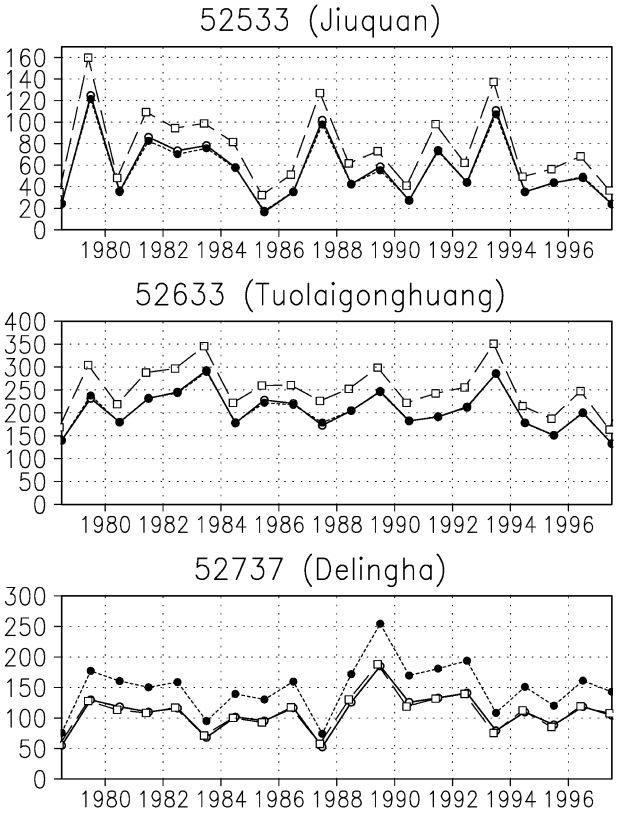

Fig. 3. Interannual variation of summertime (JJA) precipitation from 1979 to 1997at stations 52533, 53633, and 52737, which are marked "A", "B", and "C" in Fig. 1, respectively. Straight lines with open circles are the original time series. Dotted lines with closed circles are the time series of the 0.1° box of the derived product, where the station belongs to. Dashed lines with open squares are the time series of the 0.5° box of the base product, where the station belongs to. The range of the vertical axis are different each other.

of precipitation over the Qilian Mountains as well as its surrounding as areas shown in Fig. 1.

Figure 3 shows sample time series of the summer time precipitation at 52533 (104.50°E, 40.75°N, 1477.2 m), 52633 (98.42°E, 38.8°6N, 3367.0 m) and 52737 (97.37°E, 37.37°N, 2981.5 m). Time series of the Base and the Derived product where the three stations are included are also plotted in each panel of Fig. 3. In the Xie *et al.* (2004, 2006) algorithm, the orographic effect was expressed by adjusting monthly climatology against PRISM in 0.05° increments. The daily ratio to the daily climatology at each station was interpolated by using OI in 0.05° increments. Then, base (0.5°) and the Derived (0.1°) products are made from the 0.05° daily grid data. Therefore, the time series of the Base/Derived products are very similar to the original time series but are sometimes larger in magnitude, especially where the original rain-gauge data came from measurements in the valley (relatively lower elevation).

The 52533 station is located in the Hexi Corridor (Fig. 1), and it is on the north foot of the Qilian Mountains. Stations 52633 and the 52737 are located in the Qilian Mountains, but the former is on the northern slopes and latter is on the southern slopes of the Qilian Mountains (Fig. 1). Station 52533 has the smallest amount in precipitation among the three stations, but it shows the largest interannual variation.

The precipitation maxima of 52533 that match maxima of 52633 occur in the years 1979, 1989, 1990, 1993 and 1997 and these two time series show decreasing trends for the year 1978–1997. In contrast, 52737 shows the simultaneous maxima with the other two time series in 1979, 1989, and 1997, but it shows peaks of opposite direction (*i.e.,* maximum instead of minimum or vice-versa) with the other two in 1983, 1987, and 1993. These stations thus show a complex interrelationship. To address this complexity, we apply an empirical orthogonal function analysis to grasp the dominant mode of the interannual variation of the summer precipitation over this region. This is described in the next section.

A map of the linear trend pattern is shown in Fig. 4. Signs of the trends are sometimes depend on the period of the time series. To determine the impact of global climate change to the local change of the cryosphere or environmental change in historical time series, longer period analysis or dataset should be more important. In this sense, we show the trend during 1961 to 2001 where we got a consistent dataset. The Qilian Mountains and its adjacent Hexi Corridor region show an increasing trend during the 41 years. To the south of the Qilian Mountains, around the region 95°E–10°5E and 32°N–37°N, a decreasing trend is dominant. The general pattern of Fig. 4 is consistent with those of the trend pattern in summer precipitation in China for almost the same period (Zai *et al.,* 2005; Endo *et al.,* 2005).

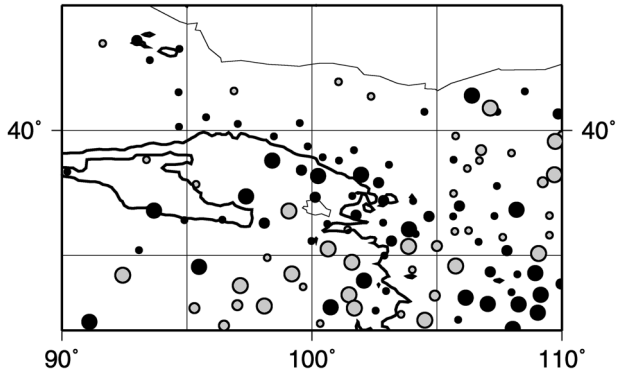

Fig. 4. Linear trends of the summer time precipitation from 1961 to 2001. Black circles indicate an increasing trend, whereas gray indicates decreasing. The magnitude of the increasing or decreasing trends are shown by the size of the circles: small size indicates 0 mm year^{-1}, medium indicates 0.5 mm year^{-1}, and large indicates 1.0 mm year^{-1}.

4. Temporal and spatial variations

The 37 stations marked in Fig. 1 were selected for the empirical orthogonal function analysis (Fig. 1). The summer time (JJA) precipitation time-series for the 41 years (1961–2001) are used as samples. A correlation matrix of the variables was used for computing the eigenvalues and eigenvectors of the EOFs because we are concerned with the interannual variability of the precipitation, not the absolute amounts. The contributions to the total variance (%) of the first five eigenvalues are 24.77, 15.84, 12.19, 7.47, and 5.15%, respectively. The first three components account for more than 50% of the total variance.

Figure 5 shows the eigenvector patterns of these first three components. The time sequence of the score for each EOF is presented in Fig. 6. The first EOF (hereafter EOF1) shows a single sign over the

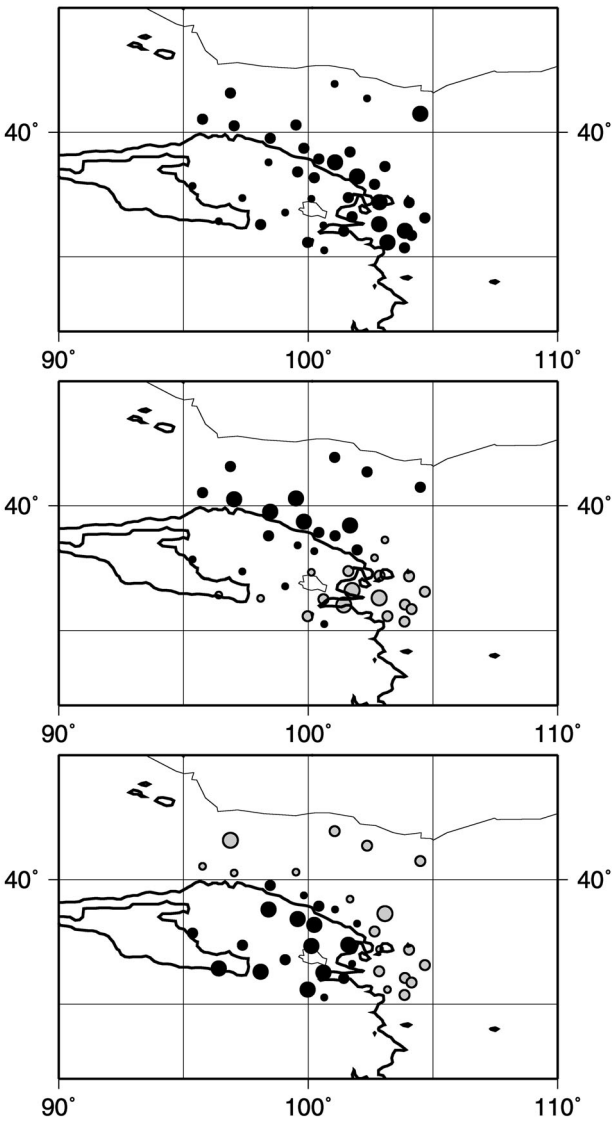

Fig. 5. Eigenvector patterns of the first three EOFs of summer time (JJA) precipitation. Positive values are black circles, negative values are gray circles.

whole domain, and stations along the Hexi Corridor and those around 103°E, 36°N have higher values than other areas. The time series of the score of the EOF1 shows gradual increasing trend and a particularly large value in the year 1979. The eigenvector pattern of EOF1 (Fig. 5 upper diagram) is similar to that of linear trend of this area (Fig. 4). However, the score of the EOF1 shows decreasing trend during 1995–2001, we need to care about the decadal change in the future.

The second EOF (EOF2) shows a clear dipole mode between northwest part of the domain and southeast part of the domain. Eigenvalues around the mountains are not large but they have positive values, which show a simultaneous signal with that of the Hexi Corridor regions in this mode. The region where EOF2 is negative corresponds to a part of the region where positive correlation was observed between the summer precipitation there and the Indian monsoon rainfall (Guo and Wang, 1988; Wang and Li, 1990; Yatagai and Yasunari, 1995). The time sequence of the score of the EOF2 (black line with open circles in the middle panel of Fig. 6) shows a clear oscillation with a period of 2–3 years. The all-India JJA time series (IMR) is also plotted in the middle panel of Fig. 6. The simultaneous correlation coefficient between the two time series is −0.46, which exceeds the 1% significant level. A clear negative relationship exists between the two time series, except for the years of 1986, 1987, and 1997. It is said that the

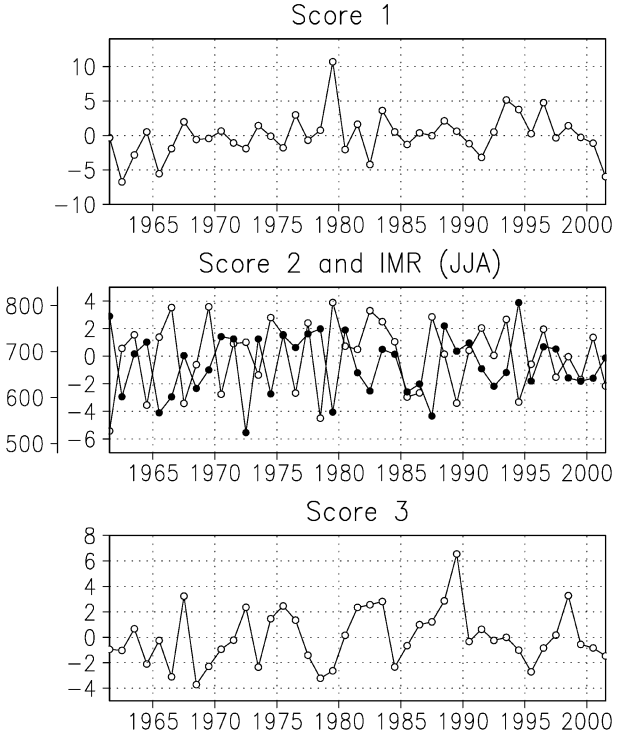

Fig. 6. Time series of the scores of the first three EOFs. The line with black circles in the middle diagram is a time series of the all India monsoon rainfall (JJA, mm).

region where eigenvector of EOF2, that is along the Hexi Corridor and a part of the Qilian Mountains, show positive values has a negative correlation between the Indian summer monsoon rainfall for JJA. Further analysis of the correlation with Indian monsoon rainfall will be discussed in the discussion section.

The third EOF shows a dominant pattern around the Qilian Mountains. Some of the Hexi Corridor stations (98°E-102°E) show a positive sign. In contrast, most stations below lower than 3000 m show negative values. This mode roughly shows a seesaw pattern between the Tibetan Plateau area and the lower (desert) area. The time series of EOFs shows an oscillation with a period between several years to several decades.

5. Relationship with the atmospheric circulation

The EOF analysis of this study clearly showed that three modes can explain the interannual precipitation variations around the Qilian Mountains. As described above, there are some dominant factors that affect the interannual variation of the precipitation anomaly of the region. Therefore, we show composite maps of the atmospheric circulation fields that correspond to each EOF. We chose the first five high and low years of EOFs (scores) to make composite charts, respectively.

Figure 7 shows the composite charts of the 500 hPa geopotential height (Z500) for the five high years (1979, 1983, 1993, 1994 and 1996) and the five low dry years (1962, 1965, 1982, 1991 and 2001) of EOF1. As shown in Figs. 5 and 6, the high years of EOF1 means wet (much precipitation) years, while the low years of EOF1 means dry (less precipitation) years. The difference of the two is also presented in Fig. 7c. Figure 7 d shows the high-low year difference of the vertically integrated water vapor flux and precipitation, which are compared to the climatological fields in Fig. 2.

EOF1 is related to the positive anomaly in west Siberia (80°E, 62°N) and the negative anomaly around Lake Baikal. The moisture flux is strengthened around the Qilian Mountains due to moisture from the west converging around this region.

Figure 8 shows the similar composite charts with Fig. 7 but for EOF2. In this mode, high years (1966, 1969, 1979, 1982 and 1987) mean much precipitation in Hexi Corridor area and less precipitation around 103°E, 36°N, and low years (1961, 1964, 1967, 1978 and 1989) shows opposite signals of the high years. A clear difference is observed in the pattern of the westerly circulation. Negative anomalies in the 500 hPa geopotential height are found at around 55°E, 65°N and 120°E, 40°N in the difference map (Fig. 8c). As a result of the circulation anomaly, the northerly moisture flux was strengthened in the wet years of the

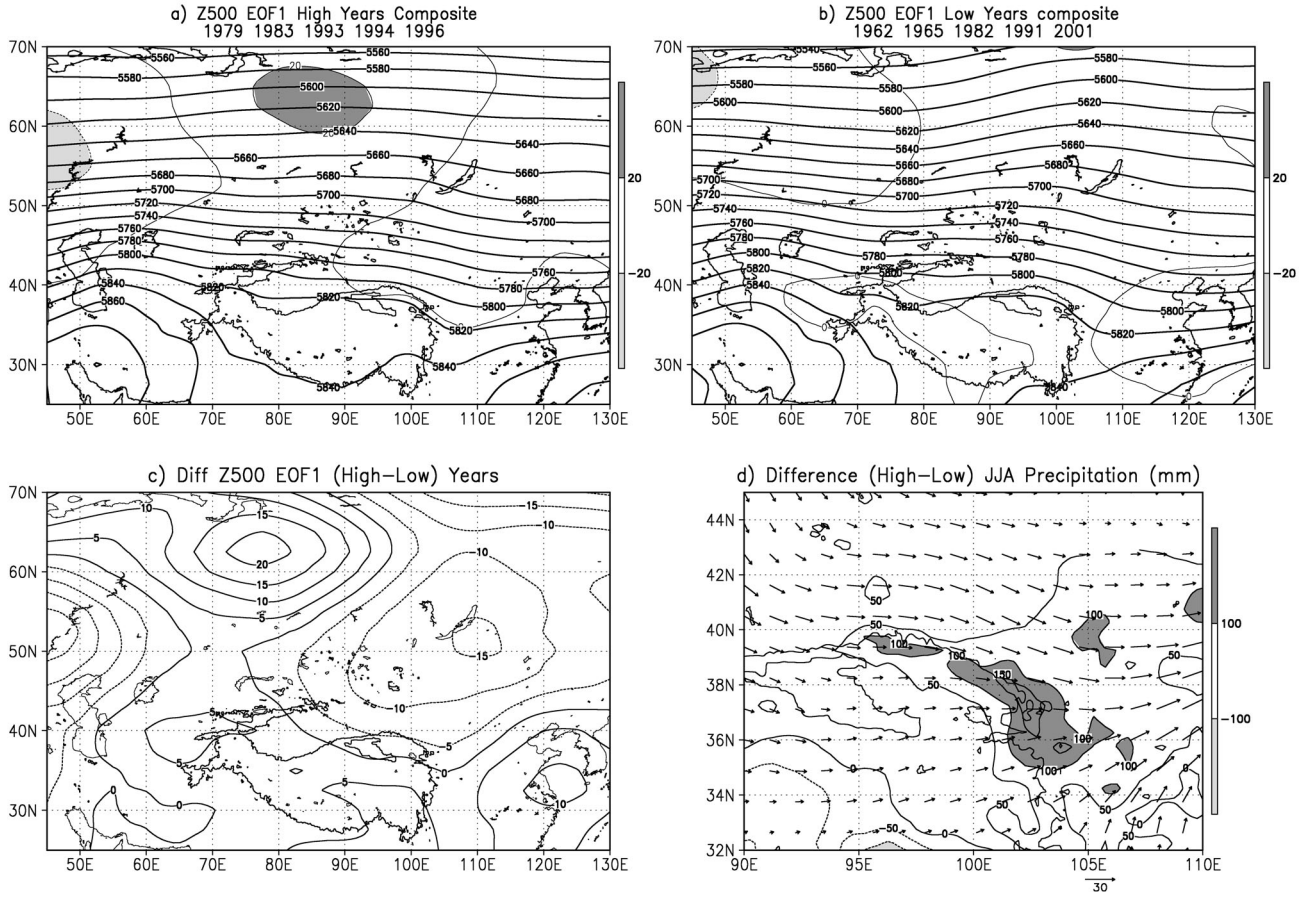

Fig. 7. (a) Composite height charts at 500 hPa for the years of largest five scores of EOF 1. The years are shown in the top of the figure. Contour interval is 20 gpm. Dark shading indicates regions in which the anomaly of the heights exceeds 20 gpm, whereas light shading indicates the anomaly negatively exceeds −20 gpm.
(b) The same as (a) but for the smallest five years. (c) Geopotential height at 500 hPa in (a) minus that in (b). Contour interval is 5 gpm. (d) Difference of the vertically integrated water vapor flux and precipitation (Base product) between the years used in (a) and (b). Shading indicates regions in which the magnitude of the precipitation difference exceeds 100 mm.

EOF2. The moisture flux shows a divergence, corresponding to the negative precipitation anomaly (102° E, 36° N and east of 105° E). It is known that the EOF2 negative region (102° E, 36° N) has more moisture from the south in the wet years for the region.

Figure 9 shows the composite charts for the EOF3 (high years: 1967, 1983, 1988, 1989 and 1998; low years: 1966, 1968, 1978, 1979 and 1995). The previous two charts of precipitation anomaly show a clear difference in the northern part of the Qilian Mountains. Here, the difference for the EOF3 shows a clear precipitation anomaly in the south of the Qilian Mountains. The difference of the Z500 field (Fig. 9c) shows a similar pattern as that of EOF1 (Fig. 7c), with a positive anomaly around 60° E, 72° N and a negative anomaly around the Lake Baikal. However, this mode (Fig. 9c) also shows a negative anomaly in the western part of the Tibetan Plateau. As a result, the moisture flux vector of southwesterly flow is strengthened over the Tibetan Plateau, and it converges in the southerly slopes of the Qilian Mountains (Fig. 9d) in the high years.

6. Disucssion

Figure 10 shows simultaneous correlation between the time series JJA precipitation of the Base product and the all India JJA precipitation. Recently, several studies pointed out that the Indian summer monsoon-ENSO relationship has been changing (Kumar *et al.,* 1999) and the impact of these signals on the East Asian monsoon has been changing (Wang *et al.,* 2001; Feng and Hu, 2004). Therefore, we presented the correlation pattern for the 41 year period (1961–2001) and the recent 25 year period (1978–2002) to IMR. Both patterns are similar to the eigenvector pattern of the EOF 2 (Fig. 5, middle panel).

Interestingly, the significant positive correlation in the northern China region of Fig. 10a (103° E,36° N; 110° E, 40° N) has disappeared in Fig. 10b. This is consistent with the findings in Feng and Hu (2004). In contrast, a significant negative correlation to the

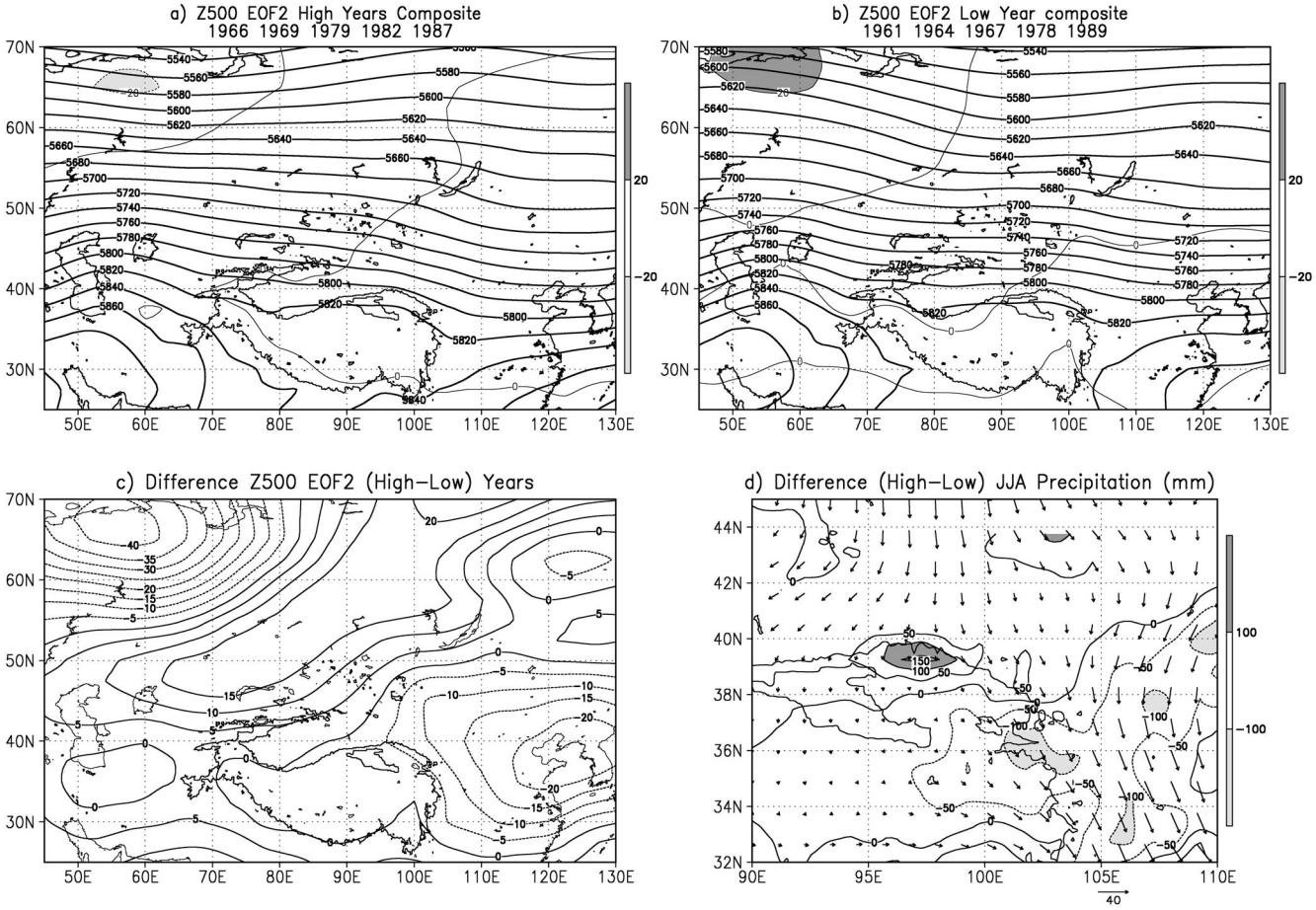

Fig. 8. The same as Fig. 8 but for EOF 2.

north of the Qilian Mountains does not disappear in Fig. 10b, rather it was strengthened. Although EOF2 shows a dipole structure in the spatial pattern, the physical mechanism between the IMR the local precipitation seems to be different from each other. Yatagai and Yasunari (1995) pointed out that a region that includes the Taklimakan Desert and the EOF2-positive region of this study showed a negative correlation to IMR, whereas a region that includes the Loess Plateau and the EOF2-negative region of this study showed a positive correlation to IMR. However, the former correlation was related to the anomaly of the westerly circulation and the latter was related to the southerly monsoon circulation.

Therefore, the correlation of ENSO with IMR and the correlation of ENSO with the precipitation anomaly of northern China (North China and the EOF2 -negative region of this study) have both weakened recently (Kumar *et al.,* 1999, Feng and Hu, 2004). However, there is another mechanism with a negative correlation between IMR and around Qilian Mountains (EOF2-positive region of this study), and this relationship has not been weakening.

We need to care that a positive correlation between an area and IMR does not mean much moisture comes from India to the area in wet years. IMR has a global (or at least continental scale) signal and IMR has significant relationship with mid-latitude circulation in interannual variation as well as intra-seasonal variation such as active/break cycle. It is considered that the mid-latitude circulation which relates to the IMR affects the interannual variation of precipitation and the moisture transport over the Qilian Mountains.

The basic method that we used in this study (an EOF analysis and composite analysis of atmospheric circulation field) was a conventional analysis method. However, both precipitation data of the target region (the Qilian Mountains) and a long-term high resolution reanalysis data have not been available till recent years. In addition, most these conventional analyses has not estimated the impact of global/continental climatic signals to local water resources, because there has not been available global/continental precipitation dataset with expressing orographic enhancement of precipitation although it is inevitably important in terms of water management and estimating accumulation on snow/glaciers. Therefore, it is keen issue to develop daily grid precipitation dataset with expressing orographic effect to achieve these purposes (Xie *et al.,* 2006).

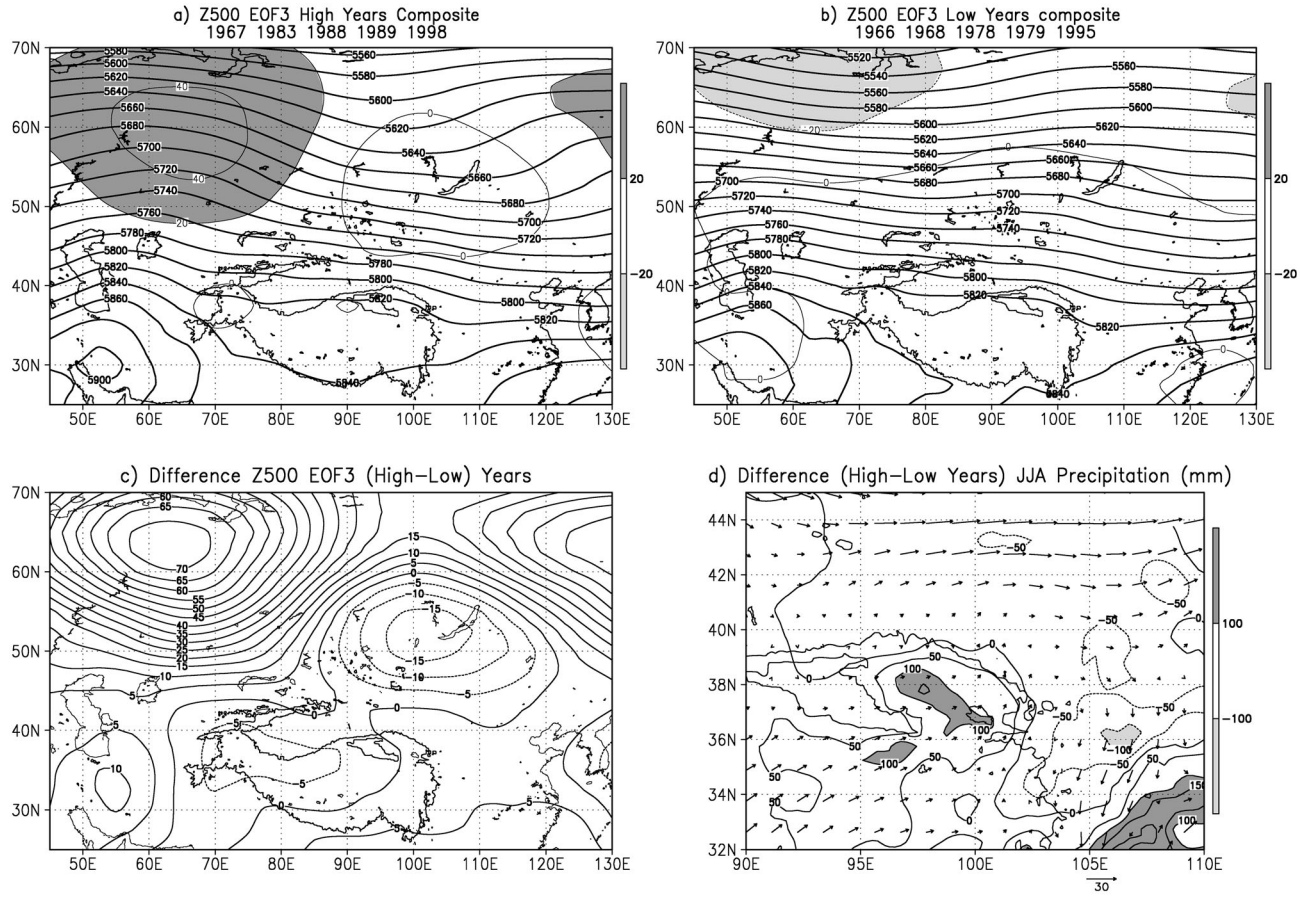

Fig. 9. The same as Fig. 8 but for EOF 3.

Recently, many attempts have been made of combining use of general circulation models and proxy data to know the past environment. However, horizontal resolution of general circulation models are generally coarse and the precipitation simulation is largely depends on the convection schemes in the models. Therefore, to understand the point proxy data, it is required to understand the regionality of precipitation variation and relationship between local precipitation and global signals such as ENSO and IMR.

However, we should be careful in change of the relationship between global signals and local precipitation as we have shown in the beginning of this section. The EOF-1 showed weak increasing trend, a peak in 1979, and decreasing trend for 1995–2001. The dominant factors of 2–3 years oscillation, decadal variation and linear trend related to the global warming are different each other. Therefore, we need to pay attention with the periodicity of the precipitation variation of this region in the future by using the updated time series.

In arid regions, precipitation case is rare. Therefore, moisture transport that related to the heavy precipitation in such region differs from the mean field (Yatagai and Yasunari, 1998). As for the target mountain region of this study which is adjacent to the arid region, diurnal cycle and orographic enhancement of precipitation should be taken into account in order to understand the variation of the precipitation record in the ice cores. Since atmospheric circulation is complicated in the target region, stable isotope technique will give us better understanding of the precipitation mechanism of this region. Combined use of isotope technique and objective reanalysis data is important for understanding the recent record of an ice core. Meteorologically, the precipitation case is rare and geography is complicated in this region, analysis of isotope in the water vapor should be essential (Yatagai *et al.,* 2004).

7. Conclusion and remarks

In order to know the time-space structure of the interannual variation of the summer time (JJA) precipitation around the Qilian Mountains, an empirical orthogonal function (EOF) analysis was applied to the JJA precipitation time of 41 years (1961–2001). The first mode showed a single mode centered along the Hexi Corridor and it shows a weakly increasing trend of precipitation. The second mode had a dipole structure between the Hexi Corridor (north of 38°N) and

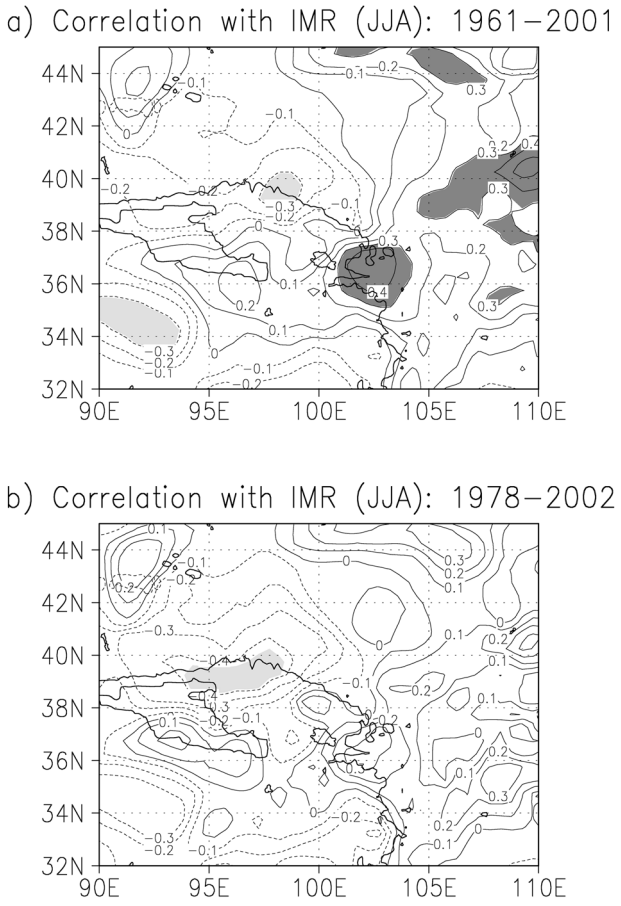

Fig. 10. (a) The correlation between summer time (JJA) precipitation and all-Indian summer monsoon (JJA). (a) For the period 1961–2001, (b) for the period 1978–2002. Dark shading indicates 95% confidence level of positive correlation, whereas light shading indicates the same level for negative correlation.

around 102.5°E, 37°N. This is correlated with the Indian summer monsoon rainfall. Namely, the Hexi Corridor and north of Qilian Mountains had a negative correlation to IMR. The third mode had a dipole structure between the plateau area and desert area.

Although there is a large altitude difference in the altitude between the Qilian Mountains and Hexi Corridor stations, the first two modes do not show a clear boundary between the two regions. Even the third mode, some of the stations in the Hexi Corridor showed the same sign with that of the Qilian Mountains. Rather, the westerly circulation anomaly is dominant factor to define the wet/dry years around this region. The northern part of the Qilian Mountains had a significant negative correlation with the IMR, and it is also related to the westerly circulation anomaly. In the southern part of the Qilian Mountains, pressure around the western part of the Tibetan Plateau and southwesterly moisture flux was also related to the interannual variation of the precipitation there.

Acknowledgments

This is a contribution from the OASIS Project (Project 4–1), being promoted by the Research Institute for Humanity and Nature. The Global Environment Research Fund (FS051 and B062) by Ministry of Environment, Japan also supported this study.

References

Chen, M., Xie, P., Janowiak, J. E. and Arkin, P. A (2002): Global land precipitation: A 50-year monthly analysis based on gauge observations. J. Hydrometeor., **3**, 249–266.

Daly, C., Neilson,R. P. and Phillips, D. L. (1994): A statistical topographic model for mapping climatological precipitation over mountainous terrain. J. Appl. Meteor., **33**, 140–158.

Ding, Y. (1994): Monsoons over China. Kluwer Academic, 419 pp.

Endo, N., Ailikun, B. and Yasunari, T. (2005): Trends in precipitation amounts and the number of rainy days and heavy rainfall events during summer in China from 1961 to 2000. J. Meteor. Soc. Japan, **83**, 621–631.

Feng, S. and Hu, Q. (2004): Variations in the teleconnection of ENSO and summer rainfall in northern China: A role of the Indian summer monsoon, J. Climate, **17**, 4871–4880.

Guo, Q.-Y. and Wang, J. (1988): A comparative study on summer monsoon in China and India. J. Tropical Meteorol., **4**, 53–60 (In Chinese with English abstract).

Kumar, K. K., Rajagopalan, B. and Cane, M. A. (1999): On the weakening relationship between the India monsoon and ENSO. Science, **284**, 2156–2159.

Nakawo, M. and Sakai, A. (2006): Change in water availability in arid regions caused by glacier changes in the mountain regions, and its impact in Central Eurasia. Global Change in Mountain Regions, SAPIENS Publishing Co. (ed. By Martin E. Price) 110–111.

Nakawo, M., Sakai, A., Naito, N. and Kato, Y. (2002): Historical evolution of the adaptability in an oasis region to water resourc changes -the scheme and the introduction of the project-. Project Report on an Oasis Region, RIHN, **2** (1) 1–13.

Numaguti, A. (1999): Origin and recycling processes of precipitating water over the Eurasian continent: Experiments using an atmospheric general circulation model, J. Geogr. Res., **104D2**, 1957–1972.

Parthasarathy, B., Munot, A. A. and Kothwale, D. R. (1995): Monthly and seasonal rainfall series for all-India homogeneous regions and meteorological subdivisions: 1871–1994. Indian Institute of Tropical Meteorology Research Rep. RR-065, Pune, India, 113 pp.

Thompson, L. G., X. Wu, E. Mosley-Thompson and Z. Xie. (1988): Climatic ice core records from the Dunde ice cap, China. Annals of Glaciology, **10**, 178–182.

Thompson, L. G., Mosley-Thompson, E., Davis, M., Bolzan, J., Dai, J., Gundestrup, N., Yao, T., Wu, X., and Xie, Z. (1989): Holocene-late Pleistocene clomatic ice core records from Qinghai-Tibetan Plateau, Science, **246**, 474–477.

Thompson, L. G., E. Mosley-Thompson, and 8 others. (1990): Glacial Stage ice core records from the subtropical Dunde ice cap, China. Annals of Glaciology, **14**, 288–297.

Thompson, L. G., Yao, T., Mosley-Thompson, E., David, M. E., Henderson, K. A. and Lin, P.-N. (2000): A high-resolution millennial record of the south Asian monsoon from Himalaya ice cores, Science, **289**, 1916–1919.

Wang, B., Wu, R. and Lau, K.-M. (2001): Interannual variability of the Asian summer monsoon: Contrasts beteen the Indian and the western North Pacific-East Aisan mon-

soons. J. Climate, **14**, 4073–4090.

Wang W.-C. and and Li, K. (1990): Precipitation fluctuation over semi arid region in Northern China and the relationship with El Nino/Southern Oscillation. J. Climate, **3**, 769–783.

Xie, P., Yatagai, A., Chen, M., Hayasaka, T., Fukushima, Y and Liu, C. (2004): An Analysis of Daily Precipitation over East Asia: Current Status and Future Improvements, Proceedings for the 6th Internationl Study Conference on GEWEX in Asia and GAME, 3–5 December, 2004, Kyoto, Japan.

Xie, P., Yatagai A., Chen M., Hayasaka T., Fukushima Y, Liu C. and Yang, S. (2006): A Gauge-Based Analysis of Daily Precipitation over East Asia, J. Hydrometeor (in press).

Yatagai, A. (2001): Estimation of precipitable water and relative humidity over the Tibetan Plateau from GMS-5 water vapor channel data, J. Meteor. Soc. Japan, **79**, 589–598.

Yatagai, A. (2003): Evaluation of hydrological balance and its variability in arid and semi-arid regions of Eurasia from ECMWF 15 year reanalysis, Hydrological Processes, **17**, 2871–2884.

Yatagai, A. and Yasunari, T. (1995): Interannual variations of summer precipitation in the arid/semi-arid regions in China and Mongolia: Their regionality and relation to the Asian summer monsoon, J. Meteor. Soc. Japan, **73**, 909–923.

Yatagai, A and Yasunari, T. (1998): Variation of Summer Water Vapor Transport over and around the Arid Region in the Interior of the Eurasian Continent. J. Meteor. Soc. Japan, **76**, 799–815.

Yatagai, A., A. Sugimoto and M. Nakawo (2004): The Isotopic Composition of Water Vapor and the Concurrent Meteorological Conditions around the Northeast Part of the Tibetan Plateau, Proceedings for the 6th Int'l Study Conference on GEWEX in Asia and GAME, December, 2004, Kyoto, Japan.

Yatagai, A., Xie, P. and Kitoh, A. (2005): Utilization of a new gauge-based daily grid precipitation dataset over monsoon Asia for a validation of daily precipitation climatology simulated by the MRI/JMA 20-km-mesh AGCM, SOLA, **1**, pp. 193–196.

Yoshimura, K., Oki, T., Ichiyanagi, K. (2004): Evaluation of two-dimensional atmospheric water circulation fields in reanalyses by using precipitation isotopes databases, J. Geophys. Res., 109, D20109, doi: 10.1029/2004JD004764.

Zai, P., Zhang, X. and Wan H., Pan X. (2005): Trends in total precipitation and frequency of daily precipitation extremes over China. J. Climate, **18**, 1096–1108.